Jian Sun
Department of Civil, Architectural and Environmental Engineering, Drexel University, Philadelphia, PA

Tomer Israeli
Department of Mechanical Engineering Ben-Gurion University of the Negev, Beer Sheva 84105, Israel

T. Agami Reddy
Department of Civil, Architectural and Environmental Engineering, Drexel University, Philadelphia, PA

Kevin Scoles
Department of Electrical and Computer Engineering, Drexel University, Philadelphia, PA

Jeffrey M. Gordon
Department of Solar Energy and Environmental Physics
Jacob Blaustein Institute for Desert Research Ben-Gurion University of the Negev, Sede Boqer Campus 84990, Israel, and
The Pearlstone Center for Aeronautical Engineering Studies
Department of Mechanical Engineering Ben-Gurion University of the Negev, Beersheva 84105, Israel

Daniel Feuermann
Department of Solar Energy and Environmental Physics
Jacob Blaustein Institute for Desert Research Ben-Gurion University of the Negev Sede Boqer Campus 84990, Israel

Modeling and Experimental Evaluation of Passive Heat Sinks for Miniature High-Flux Photovoltaic Concentrators

An important consideration in the practical realization of high-concentration photovoltaic devices is the heat rejection at high power densities to the environment. Recently, optical designs for generating solar flux in excess of 1000 suns on advanced solar cells–while respecting flux homogeneity and system compactness–were suggested with the introduction of solar fiber-optic mini-dish concentrators, tailored specifically to high-flux photovoltaic devices [1]. At the core of the design is the miniaturization of the smallest building block in the system–the concentrator and the cell–permitting low-cost mass production and reliance on passive heat rejection of solar energy that is not converted to electricity. First, this paper proposes a relatively simple 1-D axi-symmetric model for predicting the thermal and electrical performance of such mini-dish high-flux concentrators. Experimental measurements were performed with a real-sun solar simulator, indoors under controllable conditions, at flux levels up to 5,000 suns. A CFD (Computational Fluid Dynamics) model was also developed for model-validation. Both the modeling approaches predict heat sink temperatures within experimental uncertainty of a couple of degrees. Next, the 1-D axi-symmetric model is used to evaluate the sensitivity of different solar cell model assumptions, environmental effects (such as outdoor temperature, and the wind speed), heat sink size and geometry, thermal contact resistance, etc. It was confirmed that the miniaturization of the solar cell module permits passive heat rejection, such that solar cell temperatures should not reach more than 80 °C at peak insolation and stagnation conditions. Though the cell rated efficiency degrades by only 1-2% in absolute terms, higher cell temperatures may compromise the integrity of the cell circuitry and of the encapsulation. The 1-D axi-symmetric model also allows optimization of the heat sink geometric dimensions for a given volume. Hour-by-hour performance simulation results for such an optimized design configuration were performed for one month in summer and one month in winter for two locations namely Philadelphia, PA and Phoenix, AZ. The insight gained from this study is important for the proper design of the various components and materials to be used in PV mini-dishes. Equally important is that it allows similar types of analyses to be performed and well-informed design choices to be made for mini-dishes that have to operate under different climatic conditions with cells of different performance and concentration ratios. © *2005 American Institute of Physics.*
[DOI: 10.1115/1.1785799]

Introduction

Recently, a conceptual advance was proposed that represents a paradigm shift in the design of solar energy collection and delivery [1–4]. Rather than adopting the conventional wisdom of "bigger is better," the approach proposed was one of miniaturization. The collection unit is a solar fiber-optic mini-dish (Fig. 1). A small (e.g., 10–20 cm diameter) paraboloidal mirrored dish enclosure is used to concentrate solar radiation into a low-attenuation optical fiber or glass rod that transports the collected solar energy to a high-efficiency photovoltaic cell immediately behind the dish. The cell is thermally bonded to a passive cooling block. The mini-dish unit can deliver the high power densities best suited to the highest-efficiency *commercial* concentrator solar cells available (a net flux concentration of around 1000 suns) at high optical efficiency (see Fig. 2). A number of these units comprise a module that is glazed and mounted on a low-elevation dual-axis tracker. The advantages of such mini-dish designs over the classical PV concentrating designs are fully discussed in Refs. [1–3]. Preliminary experimental results and field experience from such solar fiber-optic mini-dish concentrators designed for solar surgery requiring 15,000 suns concentration have also been reported [4].

A major advantage of this design concept is that passive cooling blocks or heat sinks (as opposed to active cooling involving circulating cooling water) can suffice because of the small size of the cell (envisioned as a few square millimeters; of the order of 10–15 mm^2). The amount of heat rejection for such devices is only in the range of 10–30 W. This is a pragmatic and important benefit over the active cooling in large dish design, since this obviates the need for fail-safe mechanisms which avoid the solar cells getting compromised in case the active circulation mechanism fails.

Objectives and Problem Statement

The intent of undertaking this study is to be able to design an appropriate heat sink for the PV mini-dish. This requires a quantitative-based understanding of how solar mini-dish electrical

Contributed by the Solar Energy Division and presented at the 2004 International Solar Energy Conference of the THE AMERICAN SOCIETY OF MECHANICAL ENGINEERS. Paper number ISEC2004–65184. Manuscript received by the ASME Solar Division April 27, 2004; final revision May 4, 2004.

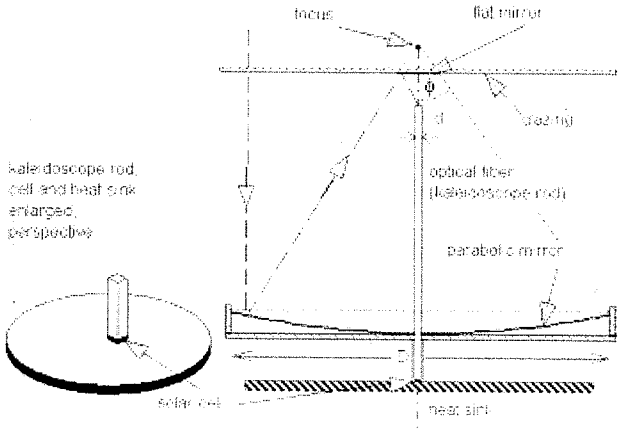

Fig. 1 Sketch of the solar mini-dish [1,2,3]

output is affected by various design variables under different climatic operating conditions. Since the efficiency of a solar cell is adversely affected by the cell temperature, the ability to model the thermal behavior of the heat sink which is thermally bonded to the solar cell is an important consideration. Equally, if not more critical, is the fact that the solar cells should not be damaged were the mini-dish to operate under open-circuit condition during which time it would attain temperatures in excess of those encountered during normal operation.

The specific objectives of this study are: (i) to propose a relatively simple computational model for determining the solar cell temperature under different passive ambient air cooling for different heat sink geometries, (ii) to validate this model both against a CFD model and against experimental results, (iii) use this model to allow determination of the optimal geometrical dimensions of the heat sink for a specified volume and the associated effect of heat sink volume, (iv) to analyze the sensitivity of various factors such as the heat sink geometry, contact thermal conductivity, etc. on cell temperature with such an optimized heat sink, and (v) to determine their effect on the monthly energy output of the mini-dish if operated in two widely different climates, namely Philadelphia, PA and in Phoenix, AZ.

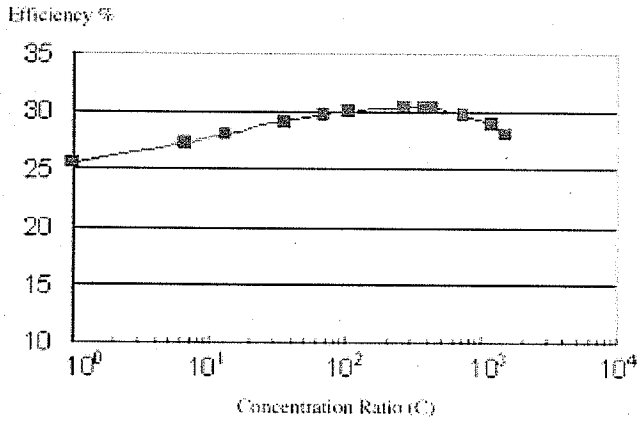

Fig. 2 Performance curve of the 3-junction $GaInP_2/GaAs/Ge$ Spectrolab cell [5]

Modeling the Mini-Dish

The solar dish assembly consists of the following elements whose performance models are required to predict the cell output during outdoor operation:

(a) The optical efficiency of the dish

We shall assume a constant value in this study of 0.89 which is considered a practical upper limit [3].

(b) The solar cell model

The published Spectrolab 3-junction solar cell performance characterized by its rated efficiency (η_{rat}) vs. concentration ratio (C) is shown for $GaInP_2/GaAs/Ge$ in Fig. 2 [5]. A regression model using the following functional form [6] has been identified from the published performance curve:

$$\eta_{rat} = a_0 + a_1 \log(C) + a_2 C^2 \tag{1}$$

with $R^2 = 0.975$ and RMSE = 0.2366.

The model parameters along with their standard errors are:

$$a_0 = 25.449 \ (\pm 0.10709), \quad a_1 = 2.1835 \ (\pm 0.07033)$$

$$\text{and } a_2 = -3.5 \times 10^{-6} \ (\pm 2.34 \times 10^{-6})$$

(c) A model to predict the cell temperature

We shall adopt the widely used expression, justified experimentally, that cell efficiency η_{cell} decreases linearly with cell temperature [6]:

$$\eta_{cell} = \eta_{rat}[1 - \beta_{cell}(T_{cell} - T_{rat})] \tag{2}$$

where β_{cell} is the cell temperature coefficient (assumed to be 0.003/°C from [5]), T_{cell} is the actual cell temperature, and T_{rat} is the rated cell temperature under reference test conditions (taken to be 20°C in this study). In principle this expression is widely used for PV modules, while in this study we shall use it for an individual cell. The temperature of the cell under actual operation is determined from a heat balance on the cell along with the fact that all absorbed radiation that is not converted into electricity must be dissipated as heat from the heat sink. Thus, an iterative process needs to be adopted to determine cell temperature.

To estimate the cooling (heat rejection) load on the solar cell, we assume: (1) high-efficiency cells such as those whose performance is shown in Fig. 2; (2) a mini-dish of 15 cm diameter; (3) concentration levels of around 1000 suns; (4) all the solar power that reaches the cell and is not converted into DC electricity must either be rejected to the cell's environment or heats the cell; and (5) the cell must be maintained below a maximum tolerance temperature of around 80°C (based on manufacturer specifications [7]). A cell temperature increase (above ambient) of 30°C (on an average) would be a sound and practical design goal from an efficiency stand point since this would reduce rated cell efficiency by only 1–2% (in absolute terms). A more critical criterion from the point of view of cell circuit integrity is to assure that the cell temperature never exceeds a threshold of about 80°C were the dish to be subject to stagnation conditions (i.e., under open-circuit operation) while being exposed to realistic but extreme climatic conditions of, say, ambient temperature of 40°C and beam irradiation of 1 kW/m^2.

Modeling the Heat Sink. The solar cell is bonded onto a mounting plate as shown in Fig. 3, which is in turn thermally bonded on a heat sink. Figure 4 shows the thermal resistance network used to model the assembly. A certain solar flux (q_c) is absorbed by the solar cell, part of which is converted to electricity and the remainder (Q) has to be rejected as heat to the environment. For the purposes of this study, we assume the following:

i. Solar cell, mounting plate and heat sink are assumed to be circular disks;
ii. Solar cell is negligible in thickness and at one uniform temperature throughout;
iii. Mounting plate is subject to heat losses from the upper face and the edge. It is treated as a lumped model;

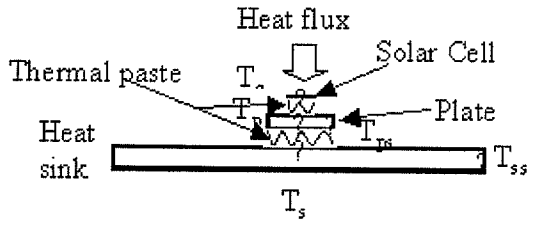

Fig. 3 Sketch of the assembly consisting of solar cell, mounting plate, and heat sink (not to scale)

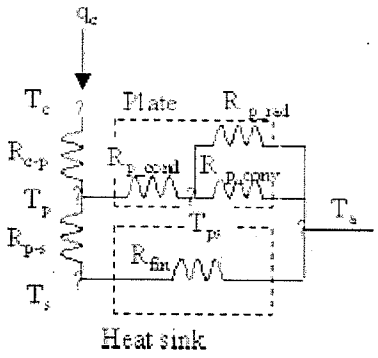

Fig. 4 Thermal resistance network showing various resistances and temperatures. R_{fin} is the equivalent thermal resistance of the heat sink calculated by Eq. (A11).

iv. Heat sink is subject to natural convective and radiative heat losses from both faces and the edge. It is modeled as 1-D axi-symmetric with an internal resistance and radiative plus convective heat resistances with uniform surface temperature.

Our modeling approach is illustrated in Figs. 3 and 4. We note that T_c is the cell temperature, T_p the temperature of the mounting plate at its center, and T_s the temperature of the heat sink at its center. T_{ps} and T_{ss} are the edge temperatures of the mounting plate and the heat sink respectively.

Details of the various correlations and the calculation procedure used to compute R_{fin} and other thermal resistances shown in Fig. 4 are given in the Appendix.

Indoor Experimental Results

Heat Sink. A heat sink was designed to accommodate a 4 ×4 mm solar cell capable of accepting 1000 suns. Under peak beam radiation of 1000 W/m^2 and for an estimated optical efficiency of 0.8, such a cell demands a collection area of about 0.02 m^2, or a primary parabolic dish with a diameter of 0.16 m. Preliminary modeling of the heat sink indicated that a circular fin of diameter 0.16 m and thickness of 0.005 m should suffice. We used standard aluminum (type 6061-T6, with a conductivity of 167 W/m/K) for the production of the fin.

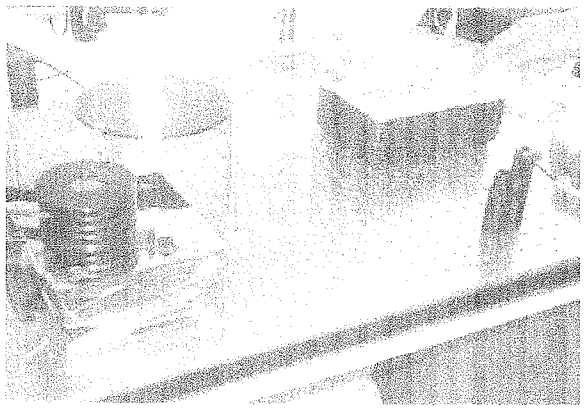

Fig. 5 The heat sink with fiber-optic delivery of concentrated sunlight inside the laboratory. Also visible are the Ophir power meter and the data acquisition system.

Solar Input. To test the performance of the heat sink, no solar cell was actually needed–the heat sink was exposed to direct solar radiation, requiring it to reject all absorbed sunlight. For this purpose, the heat sink was painted black with a high-temperature durable paint. (For outdoor operation, the fins should of course be painted white to avoid being heated by diffuse radiation). The solar absorption of the black paint was experimentally determined using a heat-up experiment [8], and was found to be 0.89 (±0.04). Rather than mounting the fin onto our mini-dish prototype, the heat sink was tested under controlled indoor conditions, using a fiber-optic mini-dish, with the fiber being guided to our indoor laboratory, projecting the sunlight onto the heat sink. This gave us full control over the ambient condition of the heat sink. Figure 5 shows the heat sink exposed to sunlight inside the laboratory. This setup ensured the relative constancy of convective heat transfer inside the laboratory. Furthermore, the setup permitted the heat sink to be exposed to varying flux concentrations. This is achieved by both varying the power input to the heat sink and by positioning the fiber tip closer to or further away from the heat sink. By positioning the fiber close to the surface of the heat

Table 1 Experimental results

Exp. No.	Configuration	Absorbed radiation (W)	Illuminated area (mm^2)	Absorbed solar flux (W/mm^2)	Temperature difference Center of heat sink—ambient (°C) Measured*	CFD Model	1-D axi-symmetric Model	Model uncertainty**
1	1 m/s air movement	2.08±0.05	2±0.5	1.04	8.8±0.2	7.9	10.3	2.5
2	No wind	2.73±0.05	2±0.5	1.37	12.4±0.2	11.4	14.7	2.0
3	No wind, lower side insulated	2.65±0.05	2±0.5	1.33	16.6±0.2	16.3	17.3	2.8
4	Same as (3) but with kaleidoscope	4.13±0.08	16±0.1	0.26	21.2±0.2	22.7	21.4	2.8

*Includes thermocouple error.
**Includes uncertainties in the measurement of incident solar radiation, absorptivity of heat sink, and illuminated cell area.

sink, flux concentrations reaching up to 5000 suns could be obtained. With the aid of a 4×4 mm dielectric kaleidoscope, the flux can be uniformly distributed over the area of the size of the cell. A power meter was used to measure the power output at the fiber exit. The power was measured before and after exposure of the heat sink. Thermocouples positioned in the central plane of the heat sink at different radii provided the temperature distribution in the heat sink. The heat sink was exposed to sunlight sufficiently long to reach steady state, typically 35 to 40 minutes. Experiments were performed during the mid-hours of the day when solar beam radiation was nearly constant. Further details of the experimental setup and results can be found in reference [8].

Results. Table 1 summarizes our validation results. Numerical calculations using a commercial 3-D numerical code, namely FIDAP [9] are also presented in the table along with results from our 1-D axi-symmetric model. To test the numerical calculation, we varied the experimental conditions by changing the illuminated area and also by reducing the heat loss via insulating the lower side of the heat sink. Agreement between measurements and calculation is reasonable and within a couple of degrees. The temperature differences between the central temperature in the disk (at half thickness) and the ambient agree with the simulation within the experimental error bars. The latter consist of the errors in temperature measurement error (0.2°C), and uncertainty in the input parameters to the simulation (i.e., measured input power (5%), estimated convective heat transfer coefficients). The numerical calculation permitted a more refined analysis of the exact temperature distribution within the heat sink. In particular, since the measurements were in the central plane of the disk, the surface (just below the solar cell) could be thoroughly explored.

Optimization of Heat Sink Dimensions

The heat sink has to be sized with a certain amount of care. If too small, the cell may attain critical temperature levels; if too large, the weight of the entire system, which may comprise of several dozens of individual dish and sink assemblies, would over-load the two-axis tracker needlessly. Heat sink optimization (involving determining the best diameter and thickness of the disk-fin for a given volume, where it is assumed that volume is proportional to costs) can be done in two ways: (i) that which maximizes heat losses from the heat sink; or (ii) that which minimizes solar cell temperature (since this would lead to maximum cell efficiency). We found the optima of both objective functions to be essentially identical. An analytical expression for the former case is derived below.

Heat loss from the heat sink assuming it to be an annular disk with inner radius r_1 and outer radius r_2 is given by:

$$Q=\frac{\theta_1}{R_{fin}} \tag{3}$$

where R_{fin} is defined by Eq. (A11) and $\theta_1=T_s-T_a$

Defining

$$u=r_2\sqrt{\beta}=r_2\sqrt{(1+\xi)\frac{2h}{kt}} \tag{4}$$

we get $r_1\sqrt{\beta}=r_1/r_2\,u$.

Further, for a heat sink of volume V, the thickness is:

$$t=\frac{V}{\pi r_2^2}$$

Substituting the above equation for t into Eq. (4), we get,

$$r_2=\left[\frac{kV}{(1+\xi)2\pi h}\right]^{1/4}u^{1/2} \tag{5}$$

and

$$r_1\sqrt{\beta}=\frac{r_1}{r_2}u=r_1\left[\frac{kV}{(1+\xi)2\pi h}\right]^{-1/4}u^{1/2} \tag{6}$$

We define

$$\varphi=\left[\frac{kV}{(1+\xi)2\pi h}\right]^{-1/4} \tag{7}$$

then,

$$r_1\sqrt{\beta}=r_1\varphi u^{1/2} \quad \text{and} \quad r_2=\varphi^{-1}u^{1/2} \tag{8}$$

Substituting Eq. (8) into Eqs. (4) and (3), the temperature difference between the center of the heat sink and the ambient becomes:

$$\theta_1=\frac{Q}{2kr_1V\varphi^3u^{-1/2}}\frac{I_1(u)K_0(Bu^{1/2})+K_1(u)I_0(Bu^{1/2})}{I_1(u)K_1(Bu^{1/2})-K_1(u)I_1(Bu^{1/2})} \tag{9}$$

where $B=r_1\varphi$

In order to determine optimal geometry of heat sink, we shall use u which is dependent on both thickness and radius of heat sink. The optimal value $u=u_0$ which maximizes the heat loss can be determined from

$$\frac{d\theta_1}{du}=0 \tag{10}$$

Though a closed form solution can be obtained, it is more convenient to determine this optimum numerically, which is what has been done in this study. Once the optimal value of u is determined for a given sink volume, the optimal diameter and thickness of the heat sink disk are easily found.

Sensitivity Analyses

The analyses which follow are based on a solar dish of 15 cm diameter with a flux concentration ratio at the cell level of $C=1000$ (excluding optical losses). Further, the following material and geometries are assumed:

i. Solar cell is 4.5 mm in diameter;
ii. Mounting plate is 30 mm in diameter, 3 mm thick, and made of copper;
iii. Heat sink is a disk made of aluminum;
iv. High conductivity paste is used between the solar cell and plate (thickness of 0.1 mm and conductivity of 60 W/m.K); while ordinary conductivity paste is used between the plate and heat sink (thickness of 0.2 mm and conductivity of 7.5 W/m.K).
v. The heat sink has an emissivity of 0.9 in the infrared, it is assumed to be painted white so as to minimize absorbed diffuse and ground-reflected radiation;

Climatic conditions assumed are:

i. direct normal radiation of 1 kW/m^2,
ii. ambient air temperature T_a of 25°C,
iii. wind velocity u_f of 5 m/s.

We shall first use the equations proposed above to study the results of the geometric optimization of the heat sink, assumed to be

Table 2 Optimal heat sink geometry for different heat sink volumes (assuming a wind velocity of 5 m/s)

Volume (cm^3)	Optimum Diameter (mm)	Optimum Thickness (mm)
5	104	0.58
10	124	0.83
15	132.5	1.09
25	148	1.44
50	175	2.10
100	204	3.05

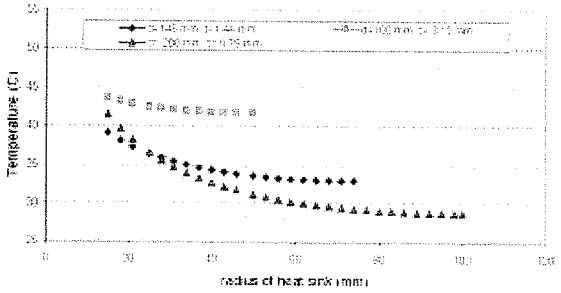

Fig. 6 Temperature distribution of three different heat sink geometries for a specified volume of 25 cm^3 assuming an ambient temperature of 25°C and wind velocity of 5 m/s. (*d*-diameter, *t*-thickness)

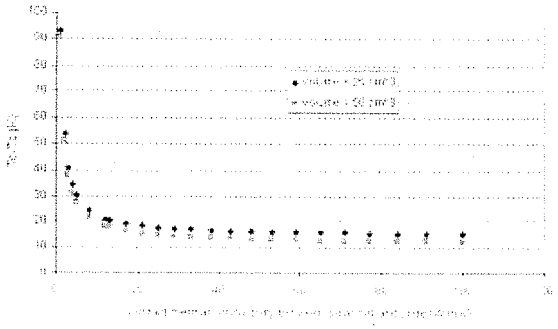

Fig. 8 Sensitivity of temperature difference between solar cell and ambient temperature for contact thermal conductivity between solar cell and mounting plate

a disk. How the optimal diameter and optimal thickness of the heat sink change for different heat sink volumes is shown in Table 2. Note the asymptotic increase of these variables with increasing heat sink volume. As we shall see in the next section, a good design range for the heat sink volume is 25–50 cm^3.

Figure 6 plots the heat sink temperature distribution along the radius of the annular heat sink for three different geometries assuming a heat sink volume of 25 cm^3. Our objective is to minimize the solar cell temperature, which also translates to a low heatsink temperature at the inner radius, i.e., at $r=15$ mm (i.e., where the mounting plate ends). We note that the temperature of the heat sink at $r=15$ mm for the optimum geometry ($d=148$ mm, $t=1.44$ mm) is lower than the other two cases ($d=100$ mm/$t=3.15$ mm and $d=200$ mm/$t=0.79$ mm) which is to be expected. Also noteworthy is the fact that the temperature difference between the three curves at $r=15$ mm is only a few degrees, indicating that the objective function has a fairly flat optimal solution.

Different wind velocities result in different optimized geometries of the heat sink. However, it is impossible to change the heat sink according to wind velocity once it has been selected and installed. So it is necessary to analyze the sensitivity of heat sink optimization to wind velocity. Figure 7 illustrates how the optimized geometry of heat sink is affected by wind velocity for two heat sink volumes. The asymptotic behavior of these plots suggests that the optimization geometry is relatively insensitive to wind speed above 3–4 m/s.

Figures 8 and 9 provide the necessary insight into the effect of contact resistance. We conclude from Fig. 8 that a contact thermal conductivity between solar cell and the mounting copper plate larger than about 20 W/m.K is adequate. From Fig. 9, we would conclude that, because of the large surface area of contact, selecting a thermal paste between the mounting plate and heat sink whose thermal conductivity exceeds 5 W/m.K would be adequate.

As discussed earlier, a critical design consideration (perhaps more crucial than the relatively small improvement in cell efficiency) is to prevent the solar cell temperature from reaching the maximum permissible temperature of 80°C in order to avoid compromising the solar cell connections and the encapsulation. The realistic worst case scenario is when the solar cell is under open-circuit operation (stagnation temperature) and exposed to a beam radiation of 1 kW/m^2 with zero wind velocity. Figure 10 shows how the stagnation temperature of the cell changes for different optimized heat sink volumes (from 5 to 100 cm^3) when ambient temperatures vary between 10–40°C. It is clear that though a heat

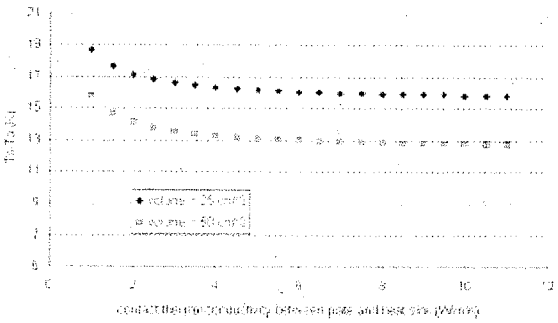

Fig. 9 Sensitivity of temperature difference between solar cell and ambient temperature for contact thermal conductivity between mounting plate and heat sink

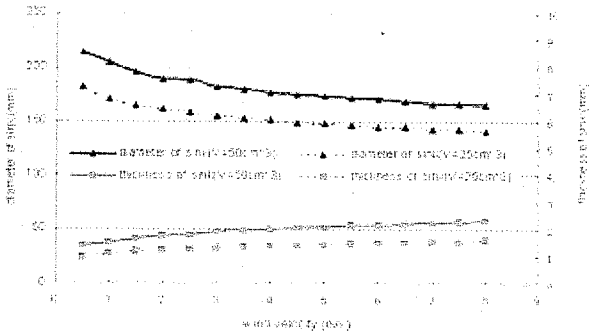

Fig. 7 Sensitivity of optimized geometry of heat sink to wind velocity for two different heat sink volumes

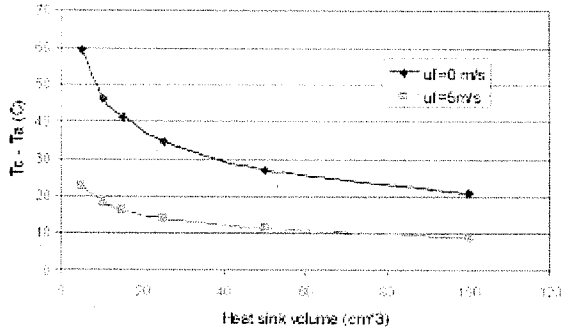

Fig. 10 Variation of solar cell temperature increase under open-circuit operation (i.e., stagnation condition) with heat sink volume under two different wind conditions. Beam irradiation of 1 kW/m^2 has been assumed. The ambient temperatures have been varied from 10°C to 40°C while generating the above figure.

Table 3 Summary of hourly simulation results using TMY data assuming 50 cm^3 heat sink volume

		Philadelphia, PA		Phoenix, AZ	
		Jan	July	Jan	July
Monthly mean ambient temperature	°C	−0.77	26.6	13.6	35.8
Monthly mean wind velocity	m/s	5.73	4.34	2.49	3.90
Amount of beam radiation received for one month	kWh/m^2	85.3	143.5	136.1	219.9
Electrical energy delivered	Wh/month	390	600	559	1078
Monthly average cell efficiency	%	29.2%	26.9%	27.6%	25.8%
Maximum cell temperature	°C	15.8	45.8	41.9	63.8

sink volume of 20 cm^3 is satisfactory from an energy view point, it would be advisable to select a heat sink volume at least 50 cm^3 in order to avoid damaging the cell.

Mini-Dish Performance Simulation Results

The optimum heat sink dimensions (for a given volume) depend on the assumed wind velocity (since it dictates the forced convection coefficient). An analysis based on the TMY data [10] for Philadelphia, PA and Phoenix, AZ (representative of a poor and a good climate respectively) during the months of January and July between the hours of 10:00 am-14:00 pm (when solar radiation is highest) revealed that mean wind velocities were between 3–6 m/s. We have assumed a value of 5 m/s in our analysis. We shall neglect the effect of spectral changes in solar beam radiation since the associated mismatch losses on a 3-junction concentration cell performance (as assumed in this study) are typically small, less than 4% at the monthly or annual level [11].

We have used the optimized heat sink geometries for different heat sink volumes ranging from 5 to 50 cm^3 shown in Table 2 to perform hourly simulations in order to determine monthly total electrical energy and the corresponding overall dish efficiency for January and July at Philadelphia and Phoenix. The simulation results are shown in Table 3. We found that increasing the heat sink volume above 10 cm^3 results in no appreciable improvement in either energy delivered or dish efficiency. However, in order not to exceed cell temperature 80°C (absolute), it would be advised to use a heat sink volume of 25 to 50 cm^3. A second observation is that the solar dish efficiency (this does not include the optical efficiency of the dish) is higher in January than July, which is due to lower ambient temperatures in January. Despite this, the total energy delivered in July is much higher (600 Wh and 1078 Wh in July as against 390 Wh and 559 Wh in January for Philadelphia and Phoenix respectively) simply because of more solar radiation availability.

Table 3 indicates that the cell temperature never exceeds 65°C even when the ambient temperature reaches 35°C. This is consistent with the experimental results presented in Ref. [11] where cell temperatures are only about 10°C higher than the environment even when relatively simple and inexpensive heat sinks are used with triple-junction cells subject to 300–500 suns. The above conclusions are also supported by experimental results reported in Ref. [12] where temperature differences are about 10–20°C for flux levels up to 10,000 suns. It also depicts how the efficiency of the cell (this does not include optical efficiency of the mini-dish) varies for the 50 cm^3 dish when operated in January and July in Philadelphia and Phoenix. We also note that the cell efficiency is about 28% in January and about 26% in July. The peak power output from the PV mini-dish is expected to be about 4 Watts.

Summary

A major advantage of PV mini-dish concentrator solar devices is that they use small solar cells which can be cooled passively. This is a pragmatic and important benefit over the active cooling in large dish design, since this obviates the need for fail-safe mechanisms which avoiding the solar cells getting compromised in case the active circulation mechanism fails. We developed a relatively simple model to predict the thermal and electrical performance of the PV mini-dish so as (i) to be able to perform sensitivity analyses of different solar cell model assumptions, environmental effects (such as outdoor temperature, and the wind speed), heat sink size and geometry, thermal contact resistance, etc; (ii) to be able to optimize the heat sink geometric dimensions for a given volume, and (iii) to determine suitable heat sink volume which would prevent the solar cell temperature from reaching the maximum permissible temperature of 80°C in order to avoid compromising the solar cell connections.

This study found that for the type of mini-dishes (15 cm diameter and 1000 concentration ratio) and 4.5 mm diameter high-efficiency solar cells assumed in this study, a good and safe design which will avoid damage to the cell even under realistic but extreme conditions would be an aluminum heat sink of 25–50 cm^3 volume and optimized dimensions of 150–175 mm diameter and 1.5–2.0 mm thickness. This study also revealed that heat sink optimization which maximizes heat losses from the heat sink yields designs essentially similar to that which minimizes solar cell temperature (since this would lead to maximum cell efficiency). We have also determined that the diameter of the fin has a broad optimum (from 130–180 mm). Wind velocity is an important influential parameter till it reaches about 3–4 m/s. Contact thermal conductivity of the paste between the solar cell and the mounting plate is also an important parameter, and must be selected such that it is at least about 20 W/m.K.

Acknowledgments

This research has been funded by the United States Department of Energy, Office of Energy Efficiency and Renewable Energy in the framework of the Concentrating Solar Power Program (Project DE-FC36-01GO11000). We would like to thank our program Officers, Lizana Pierce and Steve Sargent, for their encouragement and support.

Nomenclature

A = area, mm^2
C = geometric concentration, ratio
D = diameter, mm
k = thermal conductivity, W/m.K
h = convection heat transfer coefficient, $W/m^2.K$

$\overline{h}$ = average convection heat transfer coefficient, W/m^2.K
q = heat flux per unit area, W/m^2
Q = heat loss from heat sink, W
r = radius, mm
R = thermal resistance, K/W
R_{p_cond} = conduction thermal resistance of plate, K/W
R_{p_conv} = convective thermal resistance of plate, K/W
R_{p_rad} = radiation thermal resistance of plate, K/W
$R_{c\text{-}p}$ = contact thermal resistance between cell and plate, K/W
$R_{p\text{-}s}$ = contact thermal resistance between plate and sink, K/W
t = thickness of heat sink, mm
T = temperature, °C
T_{ps} = edge temperature of mounting plate, °C
T_{ss} = edge temperature of heat sink, °C
ΔT = temperature difference, °C
u_f = flow velocity, m/s
u = optimization parameter, (Eq. 15)
α = thermal diffusivity,m^2/s
β_{cell} = temperature coefficient for solar cell, 1/°C
ε = emissivity
σ = Stephan-Boltzman constant
ν = kinematic viscosity, m^2/s
η = efficiency of solar cell (exclusive of optical efficiency of mini-dish)
Nu = Nusselt number
Pr = Prandtl number
Ra = Rayleigh number
Re = Reynolds number

Subscripts

a = ambient
c, cell = solar cell
p = plate
s = heat sink
cp-1 = upper surface of plate
cp-2 = lower surface of plate
f = fluid
fin = heat sink
rat = rated
rad = radiative

Appendix

A sketch of the entire assembly consisting of the solar cell, mounting plate and heat sink is given by Fig. 3. The corresponding thermal network is shown in Fig. 4. The natural convection heat transfer coefficients of the upper and lower surface of the mounting plate and the heat sink is given by [13,14]:

$$h_{cp-1}=\frac{\overline{Nu}_{cp-1}k_f}{D_p} \tag{A1}$$

where

$$\overline{Nu}_{cp-1}=0.59Ra_{cp-1}^{1/4} \quad Ra_{cp-1}<10^9 \tag{A2}$$

$$\overline{Nu}_{cp-1}=0.10Ra_{cp-1}^{1/3} \quad 10^9<Ra_{cp-1}$$

$$h_{cp-2}=\frac{\overline{Nu}_{cp-2}k_f}{D_p} \tag{A3}$$

where

$$\overline{Nu}_{cp-2}=0.27Ra_{cp-2}^{1/4} 10^5<Ra_{cp-2}<10^{11} \tag{A4}$$

The natural convection coefficient of the vertical surfaces are given by similar equations, and are not reproduced here since the associated heat loss is negligible.

Table A1 Numerical values of the coefficients α_1 and α_2 with different Reynolds numbers

Re	α_1	α_2
$0-4\times10^3$	0.683	0.466
$4\times10^3-4\times10^4$	0.193	0.618
$4\times10^4-4\times10^5$	0.027	0.805

The average forced convection heat transfer coefficients of the surfaces are given by [15,16]:

$$\overline{h}_p=\frac{\overline{Nu}_p k_f}{D_p} \tag{A5}$$

where

$$\overline{Nu}_p=\alpha_1 \mathrm{Re}^{\alpha_2}\mathrm{Pr}^{1/3} \text{and } \mathrm{Re}=\frac{u_f D_p}{\nu_f} \tag{A6}$$

with α_1 and α_2 given in Table A1. These equations allow R_{p_conv} to be computed.

The internal thermal resistance of the plate can be expressed as [14]:

$$R_{p\_cond}=\frac{In(D_p/D_c)}{2\pi k_p t_p} \tag{A7}$$

The radiative heat transfer results in a significant heat loss from the plate which cannot be neglected.

We can define an equivalent linearized radiative resistance as,

$$R_{p\_rad}=\frac{1}{\varepsilon\sigma(T_{ps}^2+T_a^2)(T_{ps}+T_a)} \tag{A8}$$

We shall treat the heat sink as an annular fin (or disk) which is isothermal axially. Such a 1-D approximation is justified because of the relatively small thicknesses of both elements, which, further, are made of high conductivity materials (copper and aluminum respectively). The heat loss from such a fin can be modeled as [15,17]:

$$\frac{1}{r}\frac{d}{dr}\left(r\frac{d\theta}{dr}\right)-(1+\xi)\frac{2h}{kt}\theta=0 \quad \text{s.t.} \quad \theta(r=0)=T_p \tag{A9}$$

where $\theta=T-T_a$, and the convection coefficient h can be calculated from Eqs. (A1)–(A6).

The radiative factor is given by:

$$\xi(T,T_a)=\frac{\varepsilon\sigma(T^2+T_a^2)(T+T_a)}{h}$$

with T calculated as the average temperature of the heat sink.

The solution to Eq. (A9) is given by:

$$\frac{\theta}{\theta_s}=\frac{K_1(r_2\sqrt{\beta})I_0(r\sqrt{\beta})+I_1(r_2\sqrt{\beta})K_0(r\sqrt{\beta})}{K_1(r_2\sqrt{\beta})I_0(r_1\sqrt{\beta})+I_1(r_2\sqrt{\beta})K_0(r_1\sqrt{\beta})} \tag{A10}$$

where $\beta=(1+\xi)\,2h/kt$, $\theta_s=T_s-T_a$, I_0, I_1, K_0, K_1 are the zeroth-order Bessel functions of the first and second kind.

Subsequently, the equivalent thermal resistance, which includes both convection and linearized radiation effects, is:

$$R_{fin}=\frac{1}{2\pi tkr_1\sqrt{\beta}}\frac{I_1(r_2\sqrt{\beta})K_0(r_1\sqrt{\beta})+K_1(r_2\sqrt{\beta})I_0(r_1\sqrt{\beta})}{I_1(r_2\sqrt{\beta})K_1(r_1\sqrt{\beta})-K_1(r_2\sqrt{\beta})I_1(r_1\sqrt{\beta})} \tag{A11}$$

References

[1] Feuermann, D., and Gordon, J. M., 1999, "Solar Fiber-Optic Mini-Dishes: A New Approach to the Efficient Collection of Sunlight," Sol. Energy, 65, pp. 159–170.

[2] Feuermann, D., and Gordon, J. M., 2001, "High-Concentration Photovoltaic

Designs Based on Miniature Parabolic Dishes," Sol. Energy **70**, pp. 423–430.
[3] Reddy, T. A., Shetty, S., Jian S., Scoles, K., Eisenstein, B., Feuermann, D., and Gordon, J. M., 2003. "Preliminary Design and Experimental Results from a New Miniaturized and Modular High-Concentration Solar Photovoltaic Mini-Dish Program," report submitted to US DOE, June.
[4] Feuermann, D., Gordon, J. M., and Huleihil, M., 2002, "Solar Fiber-Optic Mini-Dish Concentrators: First Experimental Results and Field Experience," Sol. Energy, **72**, pp. 459–472.
[5] Spectrolab, 2001, Triple Junction Solar Cells, Spectrolab Inc., 12500 Gladstone Avenue, Sylmar, CA, www. Spectrolab.com
[6] Rauschenbach, H, S., 1980, *Solar Cell Array Design Handbook*, Van Nostrand Reinhold Co., New York.
[7] ISE, 2000, Fraunhofer Institute for Solar Energy Systems, Department SWT, Oltmannsstr., 5, 79100 Freiburg, Germany, (private communication).
[8] Israeli, T., 2002, Optimized Heat Sink Design and Experiments for Passive Heat Rejection of High Concentration Photovoltaic Devices, Senior Design report, Department of Mechanical Engineering, Ben-Gurion University of the Negev, Beer Sheva, 84105, Israel.
[9] FIDAP, http://www.fluent.com/software/fidap/, Fluent Software.
[10] TMY2, 1995, Typical Meteorological Years, derived from the 1961-1990 National Solar Radiation Data Base, National Renewable Energy Laboratory (NREL), Golden, CO, June.
[11] Araki, K., and Yamaguchi, M., 2003, "Influences of Spectrum Change to 3-Junction Concentrator Cells," Sol. Energy Mater. Sol. Cells, **75**, pp. 707–714.
[12] Gordon, J. M., Katz, E. A., Feuermann, D., and Huleihil, M., 2004, "Towards Ultra-High-Flux Photovoltaic Concentration," Appl. Phys. Lett., **84**(18), pp. 3642–3644.
[13] Incropera, F. P., 1999, *Liquid Cooling of Electronic Devices by Single-Phase Convection*, John Wiley, New York, NY.
[14] Lee, S., Culham, J. R., and Yovanovich, M. M., 1991, "The Effect Of Common Design Parameters on the Thermal Performance of Microelectronic Equipment: Part 1-Natural Convection," Heat Transfer in Electronic Equipment, ASME. **171**, pp. 47–54.
[15] Kaviany, M., 2002, *Principles of Heat Transfer*, 6th Edition, John Wiley & Sons, NY, NY.
[16] Culham, J. R., and Yovanovich, M. M., 2001, "Simplified Analytical Models for Forced Convection Heat Transfer From Cuboids of Arbitrary Shape," Trans. ASME, **123**, pp. 182–188.
[17] Roshenow, W. M., 1998, *Handbook of Heat Transfer*, Mc-Graw-Hill, New York, NY.